

Fast algorithms for spherical harmonic expansions, III

Mark Tygert

Courant Institute of Mathematical Sciences, NYU, 251 Mercer St., New York, NY 10012

Abstract

We accelerate the computation of spherical harmonic transforms, using what is known as the butterfly scheme. This provides a convenient alternative to the approach taken in the second paper from this series on “Fast algorithms for spherical harmonic expansions.” The requisite precomputations become manageable when organized as a “depth-first traversal” of the program’s control-flow graph, rather than as the perhaps more natural “breadth-first traversal” that processes one-by-one each level of the multilevel procedure. We illustrate the results via several numerical examples.

Keywords: butterfly, algorithm, spherical harmonic, transform, interpolative decomposition

1. Introduction

The butterfly algorithm, introduced in [9] and [10], is a procedure for rapidly applying certain matrices to arbitrary vectors. (Section 2 below provides a brief introduction to the butterfly.) The present paper uses the butterfly method in order to accelerate spherical harmonic transforms, providing an alternative to the approach in [13].

Unlike some previous works on the butterfly, the present article does not use on-the-fly evaluation of individual entries of the matrices whose applications to vectors are being accelerated. Instead, we require only efficient evaluation of full columns of the matrices, in order to make the precomputations affordable. Furthermore, efficient evaluation of full columns enables the acceleration of the application to vectors of both the matrices and their transposes. On-the-fly evaluation of columns of the matrices associated with spherical harmonic transforms is available via the three-term recurrence relations satisfied by associated Legendre functions (see, for example, Section 4 below).

The precomputations become affordable when organized as a “depth-first traversal” of the program’s control-flow graph, rather than as the perhaps more natural “breadth-first traversal” that processes one-by-one each level of the multilevel butterfly procedure (see Section 3 below).

The present article is supposed to complement [10] and [13], combining ideas from both. Although the present paper is self-contained in principle, we strongly encourage the reader to begin with [10] and [13]. The original is [9]. Major recent developments are in [3] and [15]. The introduction in [13] summarizes most prior work on computing fast spherical harmonic transforms; a new application appears in [11]. The structure of the remainder of the present article is as follows: Section 2 describes basic tools from previous works. Section 3 organizes the preprocessing for the butterfly to make memory requirements affordable. Section 4 outlines the application of the butterfly scheme to the computation of spherical harmonic transforms. Section 5 describes the results of several numerical tests. Section 6 draws some conclusions.

Throughout, we abbreviate “interpolative decomposition” to “ID” (see Subsection 2.1 for a description of the ID). The butterfly procedures formulated in [9], [10], and the present paper all use the ID for efficiency.

2. Preliminaries

In this section, we summarize certain facts from mathematical and numerical analysis, used in Sections 3 and 4. Subsection 2.1 describes interpolative decompositions (IDs). Subsection 2.2 outlines the butterfly algorithm. Subsection 2.3 summarizes basic properties of normalized associated Legendre functions.

2.1. Interpolative decompositions

In this subsection, we define interpolative decompositions (IDs) and summarize their properties.

The following lemma states that, for any $m \times n$ matrix A of rank k , there exist an $m \times k$ matrix $A^{(k)}$ whose columns constitute a subset of the columns of A , and a $k \times n$ matrix \tilde{A} , such that

1. some subset of the columns of \tilde{A} makes up the $k \times k$ identity matrix,
2. \tilde{A} is not too large, and
3. $A_{m \times k}^{(k)} \cdot \tilde{A}_{k \times n} = A_{m \times n}$.

Moreover, the lemma provides an approximation

$$A_{m \times k}^{(k)} \cdot \tilde{A}_{k \times n} \approx A_{m \times n} \quad (1)$$

when the exact rank of A is greater than k , but the $(k+1)$ st greatest singular value of A is still small. The lemma is a reformulation of Theorem 3.2 in [8] and Theorem 3 in [4]; its proof is based on techniques described in [5], [7], and [14]. We will refer to the approximation in (1) as an interpolative decomposition (ID). We call \tilde{A} the “interpolation matrix” of the ID.

Lemma 2.1. *Suppose that m and n are positive integers, and A is a real $m \times n$ matrix.*

Then, for any positive integer k with $k \leq m$ and $k \leq n$, there exist a real $k \times n$ matrix \tilde{A} , and a real $m \times k$ matrix $A^{(k)}$ whose columns constitute a subset of the columns of A , such that

1. *some subset of the columns of \tilde{A} makes up the $k \times k$ identity matrix,*
2. *no entry of \tilde{A} has an absolute value greater than 1,*
3. *the spectral norm (that is, the l^2 -operator norm) of \tilde{A} satisfies $\|\tilde{A}_{k \times n}\|_2 \leq \sqrt{k(n-k)+1}$,*
4. *the least (that is, the k th greatest) singular value of \tilde{A} is at least 1,*
5. *$A_{m \times k}^{(k)} \cdot \tilde{A}_{k \times n} = A_{m \times n}$ when $k = m$ or $k = n$, and*
6. *when $k < m$ and $k < n$, the spectral norm (that is, the l^2 -operator norm) of $A_{m \times k}^{(k)} \cdot \tilde{A}_{k \times n} - A_{m \times n}$ satisfies*

$$\|A_{m \times k}^{(k)} \cdot \tilde{A}_{k \times n} - A_{m \times n}\|_2 \leq \sqrt{k(n-k)+1} \sigma_{k+1}, \quad (2)$$

where σ_{k+1} is the $(k+1)$ st greatest singular value of A .

Properties 1, 2, 3, and 4 in Lemma 2.1 ensure that the ID $A^{(k)} \cdot \tilde{A}$ of A is numerically stable. Also, property 3 follows directly from properties 1 and 2, and property 4 follows directly from property 1.

Remark 2.2. Existing algorithms for the computation of the matrices $A^{(k)}$ and \tilde{A} in Lemma 2.1 are computationally expensive. We use instead the algorithm of [4] and [7] to produce matrices $A^{(k)}$ and \tilde{A} which satisfy slightly weaker conditions than those in Lemma 2.1. We compute $A^{(k)}$ and \tilde{A} such that

1. some subset of the columns of \tilde{A} makes up the $k \times k$ identity matrix,
2. no entry of \tilde{A} has an absolute value greater than 2,
3. the spectral norm (that is, the l^2 -operator norm) of \tilde{A} satisfies $\|\tilde{A}_{k \times n}\|_2 \leq \sqrt{4k(n-k)+1}$,
4. the least (that is, the k th greatest) singular value of \tilde{A} is at least 1,
5. $A_{m \times k}^{(k)} \cdot \tilde{A}_{k \times n} = A_{m \times n}$ when $k = m$ or $k = n$, and
6. when $k < m$ and $k < n$, the spectral norm (that is, the l^2 -operator norm) of $A_{m \times k}^{(k)} \cdot \tilde{A}_{k \times n} - A_{m \times n}$ satisfies

$$\|A_{m \times k}^{(k)} \cdot \tilde{A}_{k \times n} - A_{m \times n}\|_2 \leq \sqrt{4k(n-k)+1} \sigma_{k+1}, \quad (3)$$

where σ_{k+1} is the $(k+1)$ st greatest singular value of A .

For any positive real number ε , the algorithm can identify the least k such that $\|A^{(k)} \cdot \tilde{A} - A\|_2 \approx \varepsilon$. Furthermore, the algorithm computes both $A^{(k)}$ and \tilde{A} using at most

$$C_{\text{ID}} = O(kmn \log(n)) \quad (4)$$

floating-point operations, typically requiring only

$$C'_{\text{ID}} = O(kmn). \quad (5)$$

2.2. The butterfly algorithm

In this subsection, we outline a simple case of the butterfly algorithm from [9] and [10]; see [10] for a detailed description.

Suppose that n is a positive integer, and A is an $n \times n$ matrix. Suppose further that ε and C are positive real numbers, and k is a positive integer, such that any contiguous rectangular subblock of A containing at most Cn entries can be approximated to precision ε by a matrix whose rank is k (using the Frobenius/Hilbert-Schmidt norm to measure the accuracy of the approximation); we will refer to this hypothesis as “the rank property.” The running-time of the algorithm will be proportional to k^2/C ; C is roughly proportional to k for many matrices of interest (including discrete Fourier transforms, as is very well known), so ideally k should be small. We will say that two matrices G and H are equal to precision ε , denoted $G \approx H$, to mean that the spectral norm (that is, the l^2 -operator norm) of $G - H$ is $O(\varepsilon)$.

We now explicitly use the rank property for subblocks of multiple heights, to illustrate the basic structure of the butterfly scheme.

Consider any two adjacent contiguous rectangular subblocks L and R of A , each containing at most Cn entries and having the same numbers of rows, with L on the left and R on the right. Due to the rank property, there exist IDs

$$L \approx L^{(k)} \cdot \widetilde{L} \quad (6)$$

and

$$R \approx R^{(k)} \cdot \widetilde{R}, \quad (7)$$

where $L^{(k)}$ is a matrix having k columns, which constitute a subset of the columns of L , $R^{(k)}$ is a matrix having k columns, which constitute a subset of the columns of R , \widetilde{L} and \widetilde{R} are matrices each having k rows, and all entries of \widetilde{L} and \widetilde{R} have absolute values of at most 2.

To set notation, we concatenate the matrices L and R , and split the columns of the result in half (or approximately in half), obtaining T on top and B on the bottom:

$$\left(\begin{array}{c|c} L & R \end{array} \right) = \left(\begin{array}{c} T \\ B \end{array} \right). \quad (8)$$

Observe that the matrices T and B each have at most Cn entries (since L and R each have at most Cn entries). Similarly, we concatenate the matrices $L^{(k)}$ and $R^{(k)}$, and split the columns of the result in half (or approximately in half), obtaining $T^{(2k)}$ and $B^{(2k)}$:

$$\left(\begin{array}{c|c} L^{(k)} & R^{(k)} \end{array} \right) = \left(\begin{array}{c} T^{(2k)} \\ B^{(2k)} \end{array} \right). \quad (9)$$

Observe that the $2k$ columns of $T^{(2k)}$ are also columns of T , and that the $2k$ columns of $B^{(2k)}$ are also columns of B .

Due to the rank property, there exist IDs

$$T^{(2k)} \approx T^{(k)} \cdot \widetilde{T^{(2k)}} \quad (10)$$

and

$$B^{(2k)} \approx B^{(k)} \cdot \widetilde{B^{(2k)}}, \quad (11)$$

where $T^{(k)}$ is a matrix having k columns, which constitute a subset of the columns of $T^{(2k)}$, $B^{(k)}$ is a matrix having k columns, which constitute a subset of the columns of $B^{(2k)}$, $\widetilde{T^{(2k)}}$ and $\widetilde{B^{(2k)}}$ are matrices each having k rows, and all entries of $\widetilde{T^{(2k)}}$ and $\widetilde{B^{(2k)}}$ have absolute values of at most 2.

Combining (6)–(11) yields that

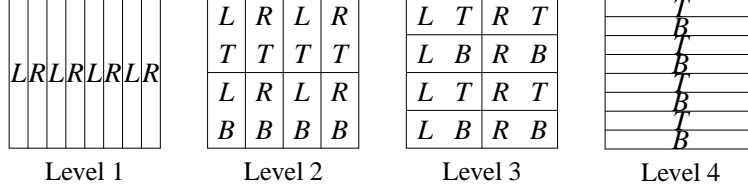
$$T \approx T^{(k)} \cdot \widetilde{T^{(2k)}} \cdot \left(\begin{array}{c|c} \widetilde{L} & \mathbf{0} \\ \hline \mathbf{0} & \widetilde{R} \end{array} \right) \quad (12)$$

and

$$B \approx B^{(k)} \cdot \widetilde{B^{(2k)}} \cdot \left(\begin{array}{c|c} \widetilde{L} & \mathbf{0} \\ \hline \mathbf{0} & \widetilde{R} \end{array} \right). \quad (13)$$

If we use m to denote the number of rows in L (which is the same as the number of rows in R), then the number of columns in L (or R) is at most Cn/m , and so the total number of entries in the matrices in the right-hand sides of (6)

Figure 1: The partitionings in the multilevel decomposition for an 8×8 matrix with $C = 1$



L indicates the left member of a pair; R indicates the right member.
 T indicates the top member of a pair; B indicates the bottom member.

and (7) can be as large as $2mk + 2k(Cn/m)$, whereas the total number of nonzero entries in the matrices in the right-hand sides of (12) and (13) is at most $mk + 4k^2 + 2k(Cn/m)$. If m is nearly as large as possible — nearly n — and k and C are much smaller than n , then $mk + 4k^2 + 2k(Cn/m)$ is about half $2mk + 2k(Cn/m)$. Thus, the representation provided in (12) and (13) of the merged matrix from (8) is more efficient than that provided in (6) and (7), both in terms of the memory required for storage, and in terms of the number of operations required for applications to vectors. Notice the advantage of using the rank property for blocks of multiple heights.

Naturally, we may repeat this process of merging adjacent blocks and splitting in half the columns of the result, updating the compressed representations after every split. We start by partitioning A into blocks each dimensioned $n \times \lfloor C \rfloor$ (except possibly for the rightmost block, which may have fewer than $\lfloor C \rfloor$ columns), and then repeatedly group unprocessed blocks (of whatever dimensions) into disjoint pairs, processing these pairs by merging and splitting them into new, unprocessed blocks having fewer rows. The resulting multilevel representation of A allows us to apply A with precision ε from the left to any column vector, or from the right to any row vector, using just $O((k^2/C) n \log(n))$ floating-point operations (there will be $O(\log(n))$ levels in the scheme, and each level except for the last will involve $O(n/C)$ interpolation matrices of dimensions $k \times (2k)$, such as $\widetilde{T}^{(2k)}$ and $\widetilde{B}^{(2k)}$). Figure 1 illustrates the resulting partitioning of A into blocks of various dimensions (but with every block having the same number of entries), when $n = 8$ and $C = 1$. For further details, see [10].

Remark 2.3. Needless to say, the same multilevel representation of A permits the rapid application of A both from the left to column vectors and from the right to row vectors. There is no need for constructing multilevel representations of both A and the transpose of A .

Remark 2.4. In practice, the IDs used for accurately approximating subblocks of A do not all have the same fixed rank k . Instead, for each subblock, we determine the minimal possible rank such that the associated ID still approximates the subblock to precision ε , and we use this ID in place of one whose rank is k . Determining ranks adaptively in this manner accelerates the algorithm substantially. For further details, see [10].

2.3. Normalized associated Legendre functions

In this subsection, we discuss several classical facts concerning normalized associated Legendre functions. All of these facts follow trivially from results contained, for example, in [1] or [12].

For any nonnegative integers l and m such that $l \geq m$, we use \overline{P}_l^m to denote the normalized associated Legendre function of degree l and order m , defined on $(-1, 1)$ via the formula

$$\overline{P}_l^m(x) = \sqrt{\frac{2l+1}{2} \frac{(l-m)!}{(l+m)!}} (1-x^2)^{m/2} \frac{d^m}{dx^m} P_l(x), \quad (14)$$

where P_l is the Legendre polynomial of degree l (see, for example, Chapter 8 of [1]). (“Normalized” refers to the fact that the normalized associated Legendre functions of a fixed order m are orthonormal on $(-1, 1)$ with respect to the standard inner product.)

The following lemma states that the normalized associated Legendre functions satisfy a certain self-adjoint second-order linear (Sturm-Liouville) differential equation.

Lemma 2.5. *Suppose that m is a nonnegative integer.*

Then,

$$-\frac{d}{dx} \left((1-x^2) \frac{d}{dx} \overline{P}_l^m(x) \right) + \left(\frac{m^2}{1-x^2} - l(l+1) \right) \overline{P}_l^m(x) = 0 \quad (15)$$

for any $x \in (-1, 1)$, and $l = m, m+1, m+2, \dots$

The following lemma states that the normalized associated Legendre function of order m and degree $m+2n$ has exactly n zeros inside $(0, 1)$, and, moreover, that the normalized associated Legendre function of order m and degree $m+2n+1$ also has exactly n zeros inside $(0, 1)$.

Lemma 2.6. *Suppose that m and n are nonnegative integers with $n > 0$.*

Then, there exist precisely n real numbers $x_0, x_1, \dots, x_{n-2}, x_{n-1}$ such that

$$0 < x_0 < x_1 < \dots < x_{n-2} < x_{n-1} < 1 \quad (16)$$

and

$$\overline{P}_{m+2n}^m(x_j) = 0 \quad (17)$$

for $j = 0, 1, \dots, n-2, n-1$.

Moreover, there exist precisely n real numbers $y_0, y_1, \dots, y_{n-2}, y_{n-1}$ such that

$$0 < y_0 < y_1 < \dots < y_{n-2} < y_{n-1} < 1 \quad (18)$$

and

$$\overline{P}_{m+2n+1}^m(y_j) = 0 \quad (19)$$

for $j = 0, 1, \dots, n-2, n-1$.

Suppose that m and n are nonnegative integers with $n > 0$. Then, we define real numbers $\rho_0, \rho_1, \dots, \rho_{n-2}, \rho_{n-1}, \sigma_0, \sigma_1, \dots, \sigma_{n-2}, \sigma_{n-1}$, and σ_n via the formulae

$$\rho_j = \frac{2(2m+4n+1)}{(1-(x_j)^2) \left(\frac{d}{dx} \overline{P}_{m+2n}^m(x_j) \right)^2} \quad (20)$$

for $j = 0, 1, \dots, n-2, n-1$, where $x_0, x_1, \dots, x_{n-2}, x_{n-1}$ are from (17),

$$\sigma_j = \frac{2(2m+4n+3)}{(1-(y_j)^2) \left(\frac{d}{dx} \overline{P}_{m+2n+1}^m(y_j) \right)^2} \quad (21)$$

for $j = 0, 1, \dots, n-2, n-1$, where $y_0, y_1, \dots, y_{n-2}, y_{n-1}$ are from (19), and

$$\sigma_n = \frac{2m+4n+3}{\left(\frac{d}{dx} \overline{P}_{m+2n+1}^m(0) \right)^2}. \quad (22)$$

The following lemma describes what are known as Gauss-Jacobi quadrature formulae corresponding to associated Legendre functions.

Lemma 2.7. *Suppose that m and n are nonnegative integers with $n > 0$.*

Then,

$$\int_{-1}^1 dx (1-x^2)^m p(x) = \sum_{j=0}^{n-1} \rho_j (1-(x_j)^2)^m p(x_j) \quad (23)$$

for any even polynomial p of degree at most $4n - 2$, where $x_0, x_1, \dots, x_{n-2}, x_{n-1}$ are from (17), and $\rho_0, \rho_1, \dots, \rho_{n-2}, \rho_{n-1}$ are defined in (20).

Furthermore,

$$\int_{-1}^1 dx (1 - x^2)^m p(x) = \sigma_n p(0) + \sum_{j=0}^{n-1} \sigma_j (1 - (y_j)^2)^m p(y_j) \quad (24)$$

for any even polynomial p of degree at most $4n$, where $y_0, y_1, \dots, y_{n-2}, y_{n-1}$ are from (19), and $\sigma_0, \sigma_1, \dots, \sigma_{n-1}, \sigma_n$ are defined in (21) and (22).

Remark 2.8. Formulae (35) and (36) of [13] incorrectly omitted the factors $(1 - (x_j)^2)^m$ and $(1 - (y_j)^2)^m$ appearing in the analogous (23) and (24) above.

Suppose that m is a nonnegative integer. Then, we define real numbers $c_m, c_{m+1}, c_{m+2}, \dots$ and $d_m, d_{m+1}, d_{m+2}, \dots$ via the formulae

$$c_l = \sqrt{\frac{(l - m + 1)(l - m + 2)(l + m + 1)(l + m + 2)}{(2l + 1)(2l + 3)^2(2l + 5)}} \quad (25)$$

for $l = m, m + 1, m + 2, \dots$, and

$$d_l = \frac{2l(l + 1) - 2m^2 - 1}{(2l - 1)(2l + 3)} \quad (26)$$

for $l = m, m + 1, m + 2, \dots$.

The following lemma states that the normalized associated Legendre functions of order m satisfy a certain three-term recurrence relation.

Lemma 2.9. Suppose that m is a nonnegative integer.

Then,

$$x^2 \bar{P}_l^m(x) = d_l \bar{P}_l^m(x) + c_l \bar{P}_{l+2}^m(x) \quad (27)$$

for any $x \in (-1, 1)$, and $l = m$ or $l = m + 1$, and

$$x^2 \bar{P}_l^m(x) = c_{l-2} \bar{P}_{l-2}^m(x) + d_l \bar{P}_l^m(x) + c_l \bar{P}_{l+2}^m(x) \quad (28)$$

for any $x \in (-1, 1)$, and $l = m + 2, m + 3, m + 4, \dots$, where $c_m, c_{m+1}, c_{m+2}, \dots$ are defined in (25), and $d_m, d_{m+1}, d_{m+2}, \dots$ are defined in (26).

3. Precomputations for the butterfly scheme

In this section, we discuss the preprocessing required for the butterfly algorithm summarized in Subsection 2.2. We will be using the notation detailed in Subsection 2.2.

Perhaps the most natural organization of the computations required to construct the multilevel representation of an $n \times n$ matrix A is first to process all blocks having n rows (Level 1 in Figure 1 above), then to process all blocks having about $n/2$ rows (Level 2 in Figure 1), then to process all blocks having about $n/4$ rows (Level 3 in Figure 1), and so on. Indeed, [10] uses this organization, which amounts to a “breadth-first traversal” of the control-flow graph for the program applying A to a vector (see, for example, [2] for an introduction to “breadth-first” and “depth-first” orderings). This scheme for preprocessing is efficient when the entries of A can be efficiently computed on-the-fly, individually. (Of course, we are assuming that A has the rank property, that is, that there are positive real numbers ε and C , and a positive integer k , such that any contiguous rectangular subblock of A containing at most Cn entries can be approximated to precision ε by a matrix whose rank is k , using the Frobenius/Hilbert-Schmidt norm to measure the accuracy of the approximation.) If the entries of A cannot be efficiently computed individually, however, then the “breadth-first traversal” may need to store $O(n^2)$ entries at some point during the precomputations, in order to avoid recomputing entries of the matrix.

If individual columns of A (but not necessarily arbitrary individual entries) can be computed efficiently, then “depth-first traversal” of the control-flow graph requires only $O((k^2/C)n \log(n))$ floating-point words of memory at

any point during the precomputations, for the following reason. We will say that we “process” a block of A to mean that we merge it with another, and split and recompress the result, producing a pair of new, unprocessed blocks. Rather than starting the preprocessing by constructing all blocks having n rows, we construct each such block only after processing as many blocks as possible which previous processing creates, but which have not yet been processed. Furthermore, we construct each block having n rows only after having already constructed (and possibly processed) all blocks to its left. We construct a block having n rows only after exhausting all possibilities for creating and processing blocks to its left.

For each *processed* block B , we need only store the interpolation matrix $\widetilde{B^{(2k)}}$ and the indices of the columns chosen for the ID; we need not store the k columns of $B^{(k)}$ selected for the ID, since the algorithm for applying A (or its transpose) to a vector never explicitly uses any columns of a block that has been merged with another and split, but instead interpolates from (or anterpolates to) the shorter blocks arising from the processing. Conveniently, the matrix $\widetilde{B^{(2k)}}$ that we must store is small – no larger than $k \times (2k)$. For each *unprocessed* block B , we do need to store the k columns in $B^{(k)}$ selected for the ID, in addition to storing $B^{(2k)}$ and the indices of the columns chosen for the ID, facilitating any subsequent processing. Although $B^{(k)}$ may have many rows, it has only as many rows as B and hence is smaller when B has fewer rows. Thus, every time we process a pair of blocks, producing a new pair of blocks having half as many rows, the storage requirements for these two pairs of blocks nearly halve. By always processing as many already constructed blocks as possible, we minimize the required amount of memory.

4. Spherical harmonic transforms via the butterfly scheme

In this section, we describe how to use the butterfly algorithm to compute fast spherical harmonic transforms, via appropriate modifications of the algorithm of [13].

We substitute the butterfly algorithm for the divide-and-conquer algorithm of [6] used in Section 3.1 of [13], otherwise leaving the approach of [13] unchanged. Specifically, given numbers $\beta_0, \beta_1, \dots, \beta_{n-2}, \beta_{n-1}$, we use the butterfly scheme to compute the numbers $\alpha_0, \alpha_1, \dots, \alpha_{n-2}, \alpha_{n-1}$ defined via the formula

$$\alpha_i = \sum_{j=0}^{n-1} \beta_j \sqrt{\rho_i} \bar{P}_{m+2j}^m(x_i), \quad (29)$$

for $i = 0, 1, \dots, n-2, n-1$, where m is a nonnegative integer, $\bar{P}_m^m, \bar{P}_{m+2}^m, \dots, \bar{P}_{m+2n-2}^m, \bar{P}_{m+2n}^m$ are the normalized associated Legendre functions of order m defined in (14), $x_0, x_1, \dots, x_{n-2}, x_{n-1}$ are the positive zeros of \bar{P}_{m+2n}^m from (17), and $\rho_0, \rho_1, \dots, \rho_{n-2}, \rho_{n-1}$ are the corresponding quadrature weights from (23). Similarly, given numbers $\alpha_0, \alpha_1, \dots, \alpha_{n-2}, \alpha_{n-1}$, we use the butterfly scheme to compute the numbers $\beta_0, \beta_1, \dots, \beta_{n-2}, \beta_{n-1}$ satisfying (29). The factors $\sqrt{\rho_0}, \sqrt{\rho_1}, \dots, \sqrt{\rho_{n-2}}, \sqrt{\rho_{n-1}}$ ensure that the linear transformation mapping $\beta_0, \beta_1, \dots, \beta_{n-2}, \beta_{n-1}$ to $\alpha_0, \alpha_1, \dots, \alpha_{n-2}, \alpha_{n-1}$ via (29) is unitary (due to (14), (23), and the orthonormality of the normalized associated Legendre functions on $(-1, 1)$), so that the inverse of the linear transformation is its transpose.

Moreover, given numbers $\nu_0, \nu_1, \dots, \nu_{n-2}, \nu_{n-1}$, we use the butterfly scheme to compute the numbers $\mu_0, \mu_1, \dots, \mu_{n-2}, \mu_{n-1}$ defined via the formula

$$\mu_i = \sum_{j=0}^{n-1} \nu_j \sqrt{\sigma_i} \bar{P}_{m+2j+1}^m(y_i), \quad (30)$$

for $i = 0, 1, \dots, n-2, n-1$, where m is a nonnegative integer, $\bar{P}_{m+1}^m, \bar{P}_{m+3}^m, \dots, \bar{P}_{m+2n-1}^m, \bar{P}_{m+2n+1}^m$ are the normalized associated Legendre functions of order m defined in (14), $y_0, y_1, \dots, y_{n-2}, y_{n-1}$ are the positive zeros of \bar{P}_{m+2n+1}^m from (19), and $\sigma_0, \sigma_1, \dots, \sigma_{n-2}, \sigma_{n-1}$ are the corresponding quadrature weights from (24). Similarly, given numbers $\mu_0, \mu_1, \dots, \mu_{n-2}, \mu_{n-1}$, we use the butterfly scheme to compute the numbers $\nu_0, \nu_1, \dots, \nu_{n-2}, \nu_{n-1}$ satisfying (30). As above, the factors $\sqrt{\sigma_0}, \sqrt{\sigma_1}, \dots, \sqrt{\sigma_{n-2}}, \sqrt{\sigma_{n-1}}$ ensure that the linear transformation mapping $\nu_0, \nu_1, \dots, \nu_{n-2}, \nu_{n-1}$ to $\mu_0, \mu_1, \dots, \mu_{n-2}, \mu_{n-1}$ via (30) is unitary, so that its inverse is its transpose.

Computing spherical harmonic transforms requires several additional computations; see [13] for details. (See also Remark 4.1 below.) The butterfly algorithm replaces only the procedure described in Section 3.1 of [13].

In order to use (29) and (30) numerically, we need to precompute the positive zeros $x_0, x_1, \dots, x_{n-2}, x_{n-1}$ of \bar{P}_{m+2n}^m from (17), the corresponding quadrature weights $\rho_0, \rho_1, \dots, \rho_{n-2}, \rho_{n-1}$ from (23), the positive zeros $y_0, y_1, \dots, y_{n-2}, y_{n-1}$ of \bar{P}_{m+2n+1}^m from (19), the corresponding quadrature weights $\sigma_0, \sigma_1, \dots, \sigma_{n-2}, \sigma_{n-1}$ from (24), and the positive zeros $z_0, z_1, \dots, z_{n-2}, z_{n-1}$ of \bar{P}_{m+2n}^m from (17).

\dots, y_{n-2}, y_{n-1} of \bar{P}_{m+2n+1}^m from (19), and the corresponding quadrature weights $\sigma_0, \sigma_1, \dots, \sigma_{n-2}, \sigma_{n-1}$ from (24). Section 3.3 of [13] describes suitable procedures (based on integrating the ordinary differential equation in (15) in “Prüfer coordinates”). We found it expedient to perform this preprocessing in extended-precision arithmetic, in order to compensate for the loss of a couple of digits of accuracy relative to the machine precision.

To perform the precomputations described in Section 3 above associated with (29) and (30), we need to be able to evaluate efficiently all n functions $\bar{P}_m^m, \bar{P}_{m+2}^m, \dots, \bar{P}_{m+2n-4}^m, \bar{P}_{m+2n-2}^m$ at any of the precomputed positive zeros $x_0, x_1, \dots, x_{n-2}, x_{n-1}$ of \bar{P}_{m+2n}^m from (17), and, similarly, we need to be able to evaluate efficiently all n functions $\bar{P}_{m+1}^m, \bar{P}_{m+3}^m, \dots, \bar{P}_{m+2n-3}^m, \bar{P}_{m+2n-1}^m$ at any of the precomputed positive zeros $y_0, y_1, \dots, y_{n-2}, y_{n-1}$ of \bar{P}_{m+2n+1}^m from (19). For this, we may use the recurrence relations (27) and (28), starting with the values of $\bar{P}_m^m(x_i), \bar{P}_{m+1}^m(y_i), \bar{P}_{m+2}^m(x_i)$, and $\bar{P}_{m+3}^m(y_i)$ obtained via (14). (We can counter underflow by tracking exponents explicitly, in the standard fashion.) Such use of the recurrence is a classic procedure; see, for example, Chapter 8 of [1]. The recurrence appears to be numerically stable when used for evaluating normalized associated Legendre functions of order m and of degrees at most $m+2n-1$, at these special points $x_0, x_1, \dots, x_{n-2}, x_{n-1}$ and $y_0, y_1, \dots, y_{n-2}, y_{n-1}$, even when n is very large. We did not need to use extended-precision arithmetic for this preprocessing.

Remark 4.1. The formula (88) in [13] that is analogous to (29) of the present paper omits the factors $\sqrt{\rho_0}, \sqrt{\rho_1}, \dots, \sqrt{\rho_{n-2}}, \sqrt{\rho_{n-1}}$ included in (29). Obviously, the vectors

$$(\alpha_0, \alpha_1, \dots, \alpha_{n-2}, \alpha_{n-1})^\top \quad (31)$$

and

$$\left(\frac{\alpha_0}{\sqrt{\rho_0}}, \frac{\alpha_1}{\sqrt{\rho_1}}, \dots, \frac{\alpha_{n-2}}{\sqrt{\rho_{n-2}}}, \frac{\alpha_{n-1}}{\sqrt{\rho_{n-1}}} \right)^\top \quad (32)$$

differ by a diagonal transformation, and so we can obtain either one from the other efficiently. In fact, the well-conditioned matrix A from Section 3.1 of [13] represents the same diagonal transformation, mapping (31) to (32). Similar remarks apply to (30), of course.

5. Numerical results

In this section, we describe the results of several numerical tests of the algorithm of the present paper.

Tables 1–4 report the results of computing from real numbers $\beta_0, \beta_1, \dots, \beta_{n-2}, \beta_{n-1}$ the real numbers $\alpha_0, \alpha_1, \dots, \alpha_{n-2}, \alpha_{n-1}$ defined by the formula

$$\alpha_i = \sum_{j=0}^{n-1} \beta_j \sqrt{\rho_i} \bar{P}_{m+2j}^m(x_i) \quad (33)$$

for $i = 0, 1, \dots, n-2, n-1$, where $\bar{P}_m^m, \bar{P}_{m+2}^m, \dots, \bar{P}_{m+2n-2}^m, \bar{P}_{m+2n}^m$ are the normalized associated Legendre functions defined in (14), $x_0, x_1, \dots, x_{n-2}, x_{n-1}$ are the positive zeros of \bar{P}_{m+2n}^m from (17), and $\rho_0, \rho_1, \dots, \rho_{n-2}, \rho_{n-1}$ are the corresponding quadrature weights from (23). We will refer to the map via (33) from $\beta_0, \beta_1, \dots, \beta_{n-2}, \beta_{n-1}$ to $\alpha_0, \alpha_1, \dots, \alpha_{n-2}, \alpha_{n-1}$ as the forward transform, and the map via (33) from $\alpha_0, \alpha_1, \dots, \alpha_{n-2}, \alpha_{n-1}$ to $\beta_0, \beta_1, \dots, \beta_{n-2}, \beta_{n-1}$ as the inverse transform (the inverse is also the transpose, due to (14), (23), and the orthonormality of the normalized associated Legendre functions on $(-1, 1)$).

Tables 5 and 6 report the results of computing from real numbers $\nu_0, \nu_1, \dots, \nu_{n-2}, \nu_{n-1}$ the real numbers $\mu_0, \mu_1, \dots, \mu_{n-2}, \mu_{n-1}$ defined by the formula

$$\mu_i = \sum_{j=0}^{n-1} \nu_j \sqrt{\sigma_i} \bar{P}_{m+2j+1}^m(y_i) \quad (34)$$

for $i = 0, 1, \dots, n-2, n-1$, where $\bar{P}_{m+1}^m, \bar{P}_{m+3}^m, \dots, \bar{P}_{m+2n-1}^m, \bar{P}_{m+2n+1}^m$ are the normalized associated Legendre functions defined in (14), $y_0, y_1, \dots, y_{n-2}, y_{n-1}$ are the positive zeros of \bar{P}_{m+2n+1}^m from (19), and $\sigma_0, \sigma_1, \dots, \sigma_{n-2}, \sigma_{n-1}$ are the corresponding quadrature weights from (24). We will refer to the map via (34) from $\nu_0, \nu_1, \dots, \nu_{n-2}, \nu_{n-1}$ to $\mu_0, \mu_1, \dots, \mu_{n-2}, \mu_{n-1}$ as the forward transform, and the map via (34) from $\mu_0, \mu_1, \dots, \mu_{n-2}, \mu_{n-1}$ to $\nu_0, \nu_1, \dots, \nu_{n-2}, \nu_{n-1}$ as the inverse transform (as above, the inverse is also the transpose).

For the test vectors β and ν whose entries appear in (33) and (34), we used normalized vectors whose entries were pseudorandom numbers drawn uniformly from $(-1, 1)$, normalized so that the sum of the squares of the entries is 1.

As described in Remark 2.4, we compute for each block in the multilevel representation of A an ID whose rank is as small as possible while still approximating the block to nearly machine precision.

The headings of the tables have the following meanings:

- n is the size of the transform, the size of the vectors α and β whose entries are given in (33), and of the vectors μ and ν whose entries are given in (34).
- m is the order of the normalized associated Legendre functions used in (33) and (34).
- k_{\max} is the maximum of the ranks of the IDs for the blocks in the multilevel representation.
- k_{avg} is the average of the ranks of the IDs for the blocks in the multilevel representation.
- k_{σ} is the standard deviation of the ranks of the IDs for the blocks in the multilevel representation.
- t_{dir} is the time in seconds required to apply an $n \times n$ matrix to an $n \times 1$ vector using the standard procedure. We estimated the last two entries for t_{dir} by multiplying the third-to-last entry in each table by 4 and 16, since the large matrices required to generate those entries cannot fit in the available 2 GB of RAM. We indicate that these entries are estimates by enclosing them in parentheses.
- t_{fwd} is the time in seconds required by the butterfly algorithm to compute the forward transform via (33) or (34), mapping from $\beta_0, \beta_1, \dots, \beta_{n-2}, \beta_{n-1}$ to $\alpha_0, \alpha_1, \dots, \alpha_{n-2}, \alpha_{n-1}$, or from $\nu_0, \nu_1, \dots, \nu_{n-2}, \nu_{n-1}$ to $\mu_0, \mu_1, \dots, \mu_{n-2}, \mu_{n-1}$.
- t_{inv} is the time in seconds required by the butterfly algorithm to compute the inverse transform via (33) or (34), mapping from $\alpha_0, \alpha_1, \dots, \alpha_{n-2}, \alpha_{n-1}$ to $\beta_0, \beta_1, \dots, \beta_{n-2}, \beta_{n-1}$, or from $\mu_0, \mu_1, \dots, \mu_{n-2}, \mu_{n-1}$ to $\nu_0, \nu_1, \dots, \nu_{n-2}, \nu_{n-1}$.
- t_{quad} is the time in seconds required in the precomputations to compute the quadrature nodes $x_0, x_1, \dots, x_{n-2}, x_{n-1}$ or $y_0, y_1, \dots, y_{n-2}, y_{n-1}$, and weights $\rho_0, \rho_1, \dots, \rho_{n-2}, \rho_{n-1}$ or $\sigma_0, \sigma_1, \dots, \sigma_{n-2}, \sigma_{n-1}$, from (23) or (24), used in (33) and (34).
- t_{comp} is the time in seconds required to construct the compressed multilevel representation used in the butterfly algorithm, after having already computed the quadrature nodes $x_0, x_1, \dots, x_{n-2}, x_{n-1}$ or $y_0, y_1, \dots, y_{n-2}, y_{n-1}$, and weights $\rho_0, \rho_1, \dots, \rho_{n-2}, \rho_{n-1}$ or $\sigma_0, \sigma_1, \dots, \sigma_{n-2}, \sigma_{n-1}$, from (23) or (24), used in (33) and (34).
- m_{\max} is the maximum number of floating-point words of memory required to store entries of the transform matrix during any point in the precomputations (all other memory requirements are negligible in comparison).
- ε_{fwd} is the maximum difference between the entries in the result of the forward transform computed via the butterfly algorithm and those computed directly via the standard procedure for applying a matrix to a vector. (The result of the forward transform is the vector α whose entries are given in (33) or the vector μ whose entries are given in (34).)
- ε_{inv} is the maximum difference between the entries in a test vector and the entries in the result of applying to the test vector first the forward transform and then the inverse transform, both computed via the butterfly algorithm. (The result of the forward transform is the vector α whose entries are given in (33) or the vector μ whose entries are given in (34). The result of the inverse transform is the vector β whose entries are given in (33) or the vector ν whose entries are given in (34).) Thus, ε_{inv} measures the accuracy of the butterfly algorithm without reference to the standard procedure for applying a matrix to a vector (unlike ε_{fwd}).

For the first level of the multilevel representation of the $n \times n$ matrix, we partitioned the matrix into blocks each dimensioned $n \times 60$ (except for the rightmost block, since n is not divisible by 60). Every block on every level has about the same number of entries (specifically, $60n$ entries). We wrote all code in Fortran 77, compiling it using the Lahey-Fujitsu Linux Express v6.2 compiler, with optimization flag `--o2` enabled. We ran all examples on one core of a 2.7 GHz Intel Core 2 Duo with 3 MB of L2 cache and 2 GB of RAM. As described in Section 4, we used extended-precision arithmetic during the portion of the preprocessing requiring integration of an ordinary differential equation, to compute quadrature nodes and weights (this is not necessary to attain high accuracy, but does yield a couple of extra digits of precision). Otherwise, our code is compliant with the IEEE double-precision standard (so that the mantissas of variables have approximately one bit of precision less than 16 digits, yielding a relative precision of about $.2\text{E-}15$).

Remark 5.1. Tables 1, 3, and 5 indicate that the transforms in (33) and (34) satisfy the rank property discussed in Subsection 2.2, with arbitrarily high precision, at least in some averaged sense. Moreover, it appears that the parameter k discussed in Subsection 2.2 can be set to be independent of the order m and size n of the transforms in (33) and (34), with the parameter C discussed in Subsection 2.2 roughly proportional to k . The acceleration provided by the butterfly algorithm thus is sufficient for computing fast spherical harmonic transforms, and is competitive with the approach taken in [13]. Unlike the approach taken in [13], the approach of the present paper does not require the use of extended-precision arithmetic during the precomputations in order to attain accuracy close to the machine precision, even while accelerating spherical harmonic transforms just as well.

Remark 5.2. The values in Tables 2, 4, and 6 vary with the size n of the transforms in (33) and (34) as expected. The values for t_{quad} are consistent with the expected values of a constant times n . The values for t_{comp} are consistent with the expected values of a constant times n^2 (with the constant being proportional to k_{avg}). The values for m_{max} are consistent with the expected values of a constant times $n \log(n)$ (again with the constant being proportional to k_{avg}); these modest memory requirements make the preprocessing feasible for large values of n such as those in the tables.

6. Conclusions

This article provides an alternative means for performing the key computational step required in [13] for computing fast spherical harmonic transforms. Unlike the implementation described in [13] of divide-and-conquer spectral methods, the butterfly scheme of the present paper does not require the use of extended precision during the compression precomputations in order to attain accuracy very close to the machine precision. With the butterfly, the required amount of preprocessing is quite reasonable, certainly not prohibitive.

Unfortunately, there seems to be little theoretical understanding of why the butterfly procedure works so well for associated Legendre functions (are the associated transforms nearly weighted averages of Fourier integral operators?). Complete proofs such as those in [10] and [13] are not yet available for the scheme of the present article. By construction, the butterfly enables fast, accurate applications of matrices to vectors when the precomputations succeed. However, we have yet to prove that the precomputations will compress the appropriate $n \times n$ matrix enough to enable applications of the matrix to vectors using only $O(n \log(n))$ floating-point operations. Nevertheless, the scheme has succeeded in all our numerical tests.

Acknowledgements

We would like to thank V. Rokhlin for his advice, for his encouragement, and for the use of his software libraries, all of which have greatly enhanced this paper and the associated computer codes. We are grateful to R. R. Coifman and Y. Shkolnisky for their interest.

Table 1: Ranks and running-times for even degrees

n	m	k_{\max}	k_{avg}	k_{σ}	t_{dir}	t_{fwd}	t_{inv}
1250	1250	170	65.3	29.5	.25E-2	.18E-2	.15E-2
2500	2500	168	67.0	32.6	.98E-2	.46E-2	.38E-2
5000	5000	195	70.5	35.9	.39E-1	.12E-1	.96E-2
10000	10000	247	73.5	38.7	.15E-0	.28E-1	.23E-1
20000	20000	308	75.9	41.5	(.60E-0)	.67E-1	.55E-1
40000	40000	379	78.0	43.8	(.24E+1)	.16E-0	.13E-0

Table 2: Precomputation times, memory requirements, and accuracies for even degrees

n	m	t_{quad}	t_{comp}	m_{\max}	ε_{fwd}	ε_{inv}
1250	1250	.46E2	.96E0	.86E6	.62E-14	.19E-13
2500	2500	.92E2	.41E1	.20E7	.37E-14	.25E-13
5000	5000	.18E3	.17E2	.50E7	.59E-14	.43E-13
10000	10000	.37E3	.82E2	.14E8	.32E-14	.57E-13
20000	20000	.74E3	.39E3	.29E8	.30E-14	.88E-13
40000	40000	.15E4	.17E4	.64E8	.24E-14	.13E-12

Table 3: Ranks and running-times for even degrees

n	m	k_{\max}	k_{avg}	k_{σ}	t_{dir}	t_{fwd}	t_{inv}
1250	0	110	67.0	23.3	.25E-2	.18E-2	.15E-2
2500	0	110	70.0	25.0	.98E-2	.48E-2	.40E-2
5000	0	111	73.9	26.1	.39E-1	.12E-1	.10E-1
10000	0	111	77.3	26.8	.15E-0	.29E-1	.24E-1
20000	0	112	80.2	27.1	(.60E-0)	.68E-1	.57E-1
40000	0	169	82.7	27.4	(.24E+1)	.16E-0	.13E-0

Table 4: Precomputation times, memory requirements, and accuracies for even degrees

n	m	t_{quad}	t_{comp}	m_{\max}	ε_{fwd}	ε_{inv}
1250	0	.44E2	.96E0	.86E6	.49E-14	.12E-12
2500	0	.88E2	.41E1	.20E7	.35E-14	.14E-12
5000	0	.18E3	.18E2	.51E7	.23E-14	.35E-12
10000	0	.36E3	.82E2	.14E8	.18E-14	.63E-12
20000	0	.74E3	.40E3	.29E8	.20E-14	.22E-11
40000	0	.14E4	.18E4	.66E8	.16E-14	.37E-11

Table 5: Ranks and running-times for odd degrees

n	m	k_{\max}	k_{avg}	k_{σ}	t_{dir}	t_{fwd}	t_{inv}
1250	1250	170	65.3	29.5	.25E-2	.17E-2	.15E-2
2500	2500	169	67.0	32.6	.98E-2	.48E-2	.39E-2
5000	5000	196	70.5	35.9	.39E-1	.12E-1	.97E-2
10000	10000	247	73.5	38.7	.15E-0	.28E-1	.24E-1
20000	20000	308	75.9	41.4	(.60E-0)	.68E-1	.56E-1
40000	40000	379	78.0	43.8	(.24E+1)	.16E-0	.13E-0

Table 6: Precomputation times, memory requirements, and accuracies for odd degrees

n	m	t_{quad}	t_{comp}	m_{\max}	ε_{fwd}	ε_{inv}
1250	1250	.46E2	.94E0	.86E6	.41E-14	.19E-13
2500	2500	.92E2	.40E1	.20E7	.41E-14	.29E-13
5000	5000	.18E3	.17E2	.50E7	.40E-14	.51E-13
10000	10000	.37E3	.80E2	.14E8	.31E-14	.62E-13
20000	20000	.74E3	.39E3	.29E8	.34E-14	.10E-12
40000	40000	.15E4	.18E4	.64E8	.25E-14	.14E-12

References

- [1] M. Abramowitz, I. A. Stegun (Eds.), Handbook of Mathematical Functions, Dover Publications, New York, 1972.
- [2] A. Aho, J. Hopcroft, J. Ullman, Data Structures and Algorithms, Addison-Wesley, 1987.
- [3] E. Candès, L. Demanet, L. Ying, A fast butterfly algorithm for the computation of Fourier integral operators, Multiscale Model. Simul. 7 (4) (2009) 1727–1750.
- [4] H. Cheng, Z. Gimbutas, P.-G. Martinsson, V. Rokhlin, On the compression of low rank matrices, SIAM J. Sci. Comput. 26 (4) (2005) 1389–1404.
- [5] S. A. Goreinov, E. E. Tyrtyshnikov, The maximal-volume concept in approximation by low-rank matrices, in: V. Olshevsky (Ed.), Structured Matrices in Mathematics, Computer Science, and Engineering I: Proceedings of an AMS-IMS-SIAM Joint Summer Research Conference, University of Colorado, Boulder, June 27–July 1, 1999, Vol. 280 of Contemporary Mathematics, AMS Publications, Providence, RI, 2001, pp. 47–51.
- [6] M. Gu, S. C. Eisenstat, A divide-and-conquer algorithm for the symmetric tridiagonal eigenproblem, SIAM J. Matrix Anal. Appl. 16 (1995) 172–191.
- [7] M. Gu, S. C. Eisenstat, Efficient algorithms for computing a strong rank-revealing QR factorization, SIAM J. Sci. Comput. 17 (4) (1996) 848–869.
- [8] P.-G. Martinsson, V. Rokhlin, M. Tygert, On interpolation and integration in finite-dimensional spaces of bounded functions, Comm. Appl. Math. Comput. Sci. 1 (2006) 133–142.
- [9] E. Michielssen, A. Boag, A multilevel matrix decomposition algorithm for analyzing scattering from large structures, IEEE Trans. Antennas and Propagation 44 (8) (1996) 1086–1093.
- [10] M. O’Neil, F. Woolfe, V. Rokhlin, An algorithm for the rapid evaluation of special function transforms, Appl. Comput. Harmon. Anal. In press.
- [11] M. G. Reuter, M. A. Ratner, T. Seideman, A fast method for solving both the time-dependent Schrödinger equation in angular coordinates and its associated “ m -mixing” problem, J. Chem. Phys. 131 (2009) 094108–1 — 094108–6.
- [12] G. Szegő, Orthogonal Polynomials, 11th Edition, Vol. 23 of Colloquium Publications, American Mathematical Society, Providence, RI, 2003.
- [13] M. Tygert, Fast algorithms for spherical harmonic expansions, II, J. Comput. Phys. 227 (8) (2008) 4260–4279.
- [14] E. E. Tyrtyshnikov, Incomplete cross approximation in the mosaic-skeleton method, Computing 64 (4) (2000) 367–380.
- [15] L. Ying, Sparse Fourier transform via butterfly algorithm, SIAM J. Sci. Comput. 31 (3) (2009) 1678–1694.